npj | climate and atmospheric science

www.nature.com/npjclimatsci

ARTICLE OPEN

Check for updates

Chemistry, street canyon geometry, and emissions effects on NO_2 "hotspots" and regulatory "wiggle room"

Yuqing Dai[1], Xiaoming Cai[1], Jian Zhong[1] and A. Robert MacKenzie[1]✉

The extent to which nitrogen dioxide (NO_2) undergoes complex chemical-transport processes near strong nitrogen-oxide sources in street canyons is not fully understood. A multi-box framework with volatile organic compound (VOC) chemistry has been evaluated against large-eddy simulation (LES) data and observations, and then used to simulate NO_2 at street-canyon "hotspots". 42,000 sensitivity studies — varying nitrogen oxides (NO_x) and VOC emission strength, and primary NO_2 fraction (f_{NO_2}) emitted within each of five streetscape cases — show the importance of detailed VOC chemistry, even in regular canyons (aspect ratio, AR = 1) when the ambient wind is weak. For a midsummer central London scenario, the inclusion of chemistry moves the canyon from compliance to out-of-compliance with the 1-hour NO_2 standard. Ignoring street-canyon chemistry can lead, therefore, to false positives in regulatory air quality modelling. Neglecting VOC chemistry can underestimate NO_2 by 6–22% in regular canyons, and even more (−51–31%) in deep canyons (AR = 2), particularly with lower f_{NO_2} values resulting from gasoline-dominated vehicle fleets or by tighter control of primary NO_2 from diesels. The very significant changes in regulatory "wiggle room" across sensitivity studies demonstrate the utility of this kind of chemistry-transport modelling for identifying efficient and effective regulatory pathways.

npj Climate and Atmospheric Science (2022)5:102 ; https://doi.org/10.1038/s41612-022-00323-w

INTRODUCTION

Poor outdoor air quality has been linked to a mortality burden of between 28,000 and 36,000 every year in the UK[1] and 4.2 million deaths brought forward globally[2]; it also significantly increases the risk of respiratory diseases and has impacts on cognitive performance in particular with vulnerable groups[3–5]. Nitrogen dioxide (NO_2) is one of the most harmful urban air pollutants, with direct adverse impacts on human health; it also contributes to the formation of harmful secondary pollutants such as ozone (O_3), peroxyacetyl nitrate (PAN), and particulate matter (PM). PAN, in turn, is important as a "reservoir" compound, transporting and then releasing reactive nitrogen downstream of its sources[6,7].

Tail-pipe emissions from internal combustion engines are the dominant primary source of NO_2 in most urban areas[8]. Subsequently, secondary NO_2 is generated from nitric oxide (NO) through its rapid reactions with O_3, hydroperoxy (HO_2), and organic peroxyl radicals (RO_2). The radicals are generated from the photo-oxidation of volatile organic compounds (VOCs), which derive predominantly from tail-pipe emissions in cold conditions[9,10], augmented by evaporative[11,12] and biogenic emissions[13–15] in warmer conditions. For cities in the global North, traffic emissions are estimated to be responsible for more than 60% of NO_x concentrations at the roadside in urban areas[16–18]. Although prominent downward trends in the annual NO_2 concentrations have been observed in many megacities (e.g., London, Beijing) under tight emission control strategies, evidence indicates that there is no safe threshold of exposure to air pollutants[19] and the Global Air Quality Guidelines (AQGs) have been updated by the World Health Organization (WHO) in 2021, suggesting that annual NO_2 levels should not exceed 10 μg m^{-3} (a 75% reduction), while the 1-hour limit (200 μg m^{-3}) remains valid[20]. Breaches of NO_2 levels against standards still occurred in congested areas with inadequate ventilation (i.e., regions with poor mixing with the overlying atmosphere — "street canyons" for example). More residents in urban areas will be affected by air quality issues as buildings in urban areas become denser[21] and as urban populations increase[22].

The term "street canyon" refers to a narrow street flanked by continuous in-line buildings[23]. According to the aspect ratio (AR, the ratio of building height to street width), street canyons can be categorized as "avenue" (AR ≤ 0.5), "regular" (AR ≈ 1), and "deep" (AR ≥ 2) canyons[24]. Previous wind/water-tunnel-scale studies found that one vortex and multiple counter-rotated vortexes in idealised regular and deep urban canyons with symmetrical geometries, flat roofs, and a high Reynold (Re) number (~10^6), respectively[25,26]. However, there is a continuing debate about the threshold value for the formation of multi-vortexes and Re-independence in street canyons. Chew, et al.[27] reported that a single vortex may form in the deep canyon (c.f., AR = 2) if Re is around 10^5; full-scale urban canyon simulations showed that only a primary vortex is generated in street canyons with AR equals to one and three, and two vortexes are formed when AR equals to five and six, while the essential Re for Re-independent airflows is ~10^6 and ~10^7 for canyons with AR = 3 and AR = 5, respectively[28,29]. These controversies suggest that CFD results should be re-visited in the future by comparison with observations and are beyond the scope of this study.

NO_2 builds up in heavily trafficked street canyons because of intensive vehicle emissions and the inefficient exchange of air with the ambient background aloft. This exchange of air, or ventilation, has been quantified as a rate with units of velocity, called a "transfer velocity"[30], "air ventilation rate"[31], or "exchange velocity"[26]. The distribution of NO_2 in street canyons is complicated by chemical reactions. NO, NO_2, and O_3 rapidly adjust towards a photo-stationary state (see, for example, Hewitt and Jackson[32], Baker, et al.[33]) (Supplementary Methods, reactions 10 and 11). As air flows around urban street canyons, NO_x (i.e., the sum of NO and NO_2)-O_3 and organic free-radical chemistry

[1]School of Geography, Earth & Environmental Sciences, University of Birmingham, Edgbaston, Birmingham B15 2TT, UK. ✉email: a.r.mackenzie@bham.ac.uk

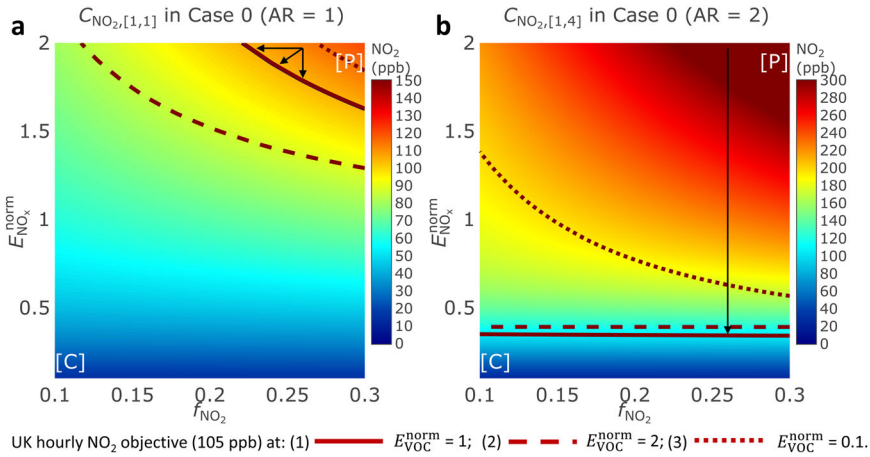

Fig. 1 Emissions effects on upward-vortex side NO_2 mixing-ratios at the pedestrian level in urban canyons. The upward-vortex side NO_2 mixing-ratios (ppb) at the pedestrian level of the regular (**a**) and deep (**b**) canyons at $E^{norm}_{VOCs} = 1$ in Case 0 ($U_0 = 2\ m\ s^{-1}$). f_{NO_2} is the primary NO_2 fraction, $E^{norm}_{NO_x}$ and E^{norm}_{VOCs} are the ratios of NO_x and VOC emission rates to their typical emission condition (TEC), respectively. All simulated patterns change when E_{VOCs} is changed, and the compliance line shifts to the dotted and dashed lines when E^{norm}_{VOCs} changes to 0.1 and 2, respectively. The regions "[P]" and "[C]" divided by the compliance line represent the polluted and clean air zone, respectively. The arrows represent control strategies for NO_2 reduction under an intense emission condition (IEC), see text for details.

(hereafter denoted as "free-radical chemistry") also take place. Previous studies have stressed the critical role of VOC abatement and hence free-radical chemistry in controlling NO_2 and O_3 in VOC-sensitive urban areas at the regional scale[34–36]. However, the impact of VOC on NO_2 concentrations at the street scale has been very sparingly studied. Computational fluid dynamics (CFD)-based models such as Reynolds-averaged Navier-Stokes (RANS) and large eddy simulation (LES) have very occasionally been used for simulating reactive species (e.g., NO, NO_2, O_3) in street canyons by coupling dynamics and chemistry[33,37–41]. These models can provide very detailed airflow characteristics and a very high-resolution distribution of reactive species in street canyons[37,42,43]. Nevertheless, it is difficult to incorporate complex chemical schemes into these simulations due to computational resource constraints, very substantially restricting their scope to survey the parameter space through sensitivity studies. Gaussian models can be extended to allow fast computation of the dispersion of pollutants within street canyons, but they are less process-based and have limited ability to represent complex chemical reactions in the atmosphere. Although single-box models (e.g., Pugh, et al.[44]) allow more complicated chemistry and/or microphysics to be incorporated, they cannot calculate within-canyon concentration gradients and chemical segregation[45–48], which gives rise to highly localized pollution "hotspots".

In the present study, we used a two-dimensional (2D) multi-box framework that removes the well-mixed assumption presented in the single-box calculation, to simulate NO_2 mixing ratios within urban street canyons. VOC chemistry was incorporated into the model without an unmanageable loss of computational speed[49]. Overall, the model offers the spatial distribution of pollutants with a fairly short computational time (e.g., ~6 min for a deep canyon and ~3 min for a regular canyon) compared to the LES (~10 days). Here, the model results at the pedestrian level were evaluated against available observations. By taking into account a large portfolio of emission scenarios, different routes for reducing NO_2 in street canyons were explored. The model results show the extent to which it is important to include free-radical chemistry, as distinct from the purely inorganic NO_x-O_3 scheme, thereby supporting strategies for efficient and effective air pollutant management.

This article is organized as follows: the Methods section comprises three sub-sections, i.e. "model description" describes the multi-box model used in this work and its basic components; "model evaluation" compares the model results to measurements within four realistic street canyons; "model scenarios" presents the details of the model configuration for different emission and meteorological scenarios. Three sub-sections in the Results and Discussion section demonstrate the analysed results in street canyons, the influence of emission heterogeneity and meteorology on model results, and implications for future modelling and air quality regulatory policy, respectively.

RESULTS AND DISCUSSION

NO_2 response surfaces and air quality management

Figure 1 shows the modelled mixing ratios of NO_2 on the upward-flowing side of the main circulatory vortex, at the pedestrian level of regular and deep street canyons. The figure shows a 2D slice through the parameter space at the typical VOC emission rate ($E^{norm}_{VOCs} = 1$) and $U_0 = 2\ m\ s^{-1}$. The solid line dividing the polluted air zone (P) and the clean air zone (C) is the UK hourly air quality objective for NO_2 (105 ppb corresponding to 200 μg m^{-3} based on the conversion factor estimated at 20 °C and 1 atm), which we will describe below as the "compliance line". The dotted and dashed lines show the compliance line from other relative VOC emission values projected onto the $E^{norm}_{VOCs} = 1$ surface: we refer to the dotted $E^{norm}_{VOCs} = 0.1$ compliance line as the "low free-radical chemistry" line (i.e., more complicated chemistry is essentially near-absent, as in most current regulatory models), and the dashed $E^{norm}_{VOCs} = 2$ as the "intense free-radical chemistry" line. The compliance lines reveal a complex relationship between emission factors and free-radical chemistry. It should of course be borne in mind that increases or decreases in NO_x and VOC emissions as well as changes in primary NO_2 are often simultaneous in reality, but the lines in Fig. 1 show the extent to which compliance with the air quality standard depends on assumptions about chemistry that are routinely absent from regulatory modelling. Similarly, the much more computationally intensive LES might typically investigate 6 or 10 of the 8400 scenarios tested by the multi-box model (e.g., Kwak and Baik[50], Kim, et al.[51], Kwak, et al.[52]), and so could miss the general patterns captured in Fig. 1.

The impact of emissions and primary NO_2 in the presence of free VOC radical chemistry presents a challenge to policymakers pursuing effective mitigation options. Consider a regular canyon with an intense emission condition (IEC) of 3000 vehicle hr^{-1} with $E^{norm}_{NO_x} = 2$ and $f_{NO_2} = 0.26$ (with $E^{norm}_{VOCs} = 1$ for illustration purposes

in Fig. 1a), that is, modelling a putatively perfect AR = 1 canyon in Marylebone Road in central London. Under these conditions, the site is not compliant: the site conditions are above and to the right of the compliance line (Fig. 1a). NO_2 mixing-ratio reductions are then strongly dependent upon total NO_x emissions and f_{NO_2}. Reducing solely E_{NO_x} by ~10% (the horizontal arrow) or f_{NO_2} from 0.26 to 0.23 (the vertical arrow) brings NO_2 into compliance. However, if free-radical chemistry is effectively ignored, the site is below and to the left of the dashed line and so already in compliance. This would be, in effect, a false positive outcome arising from the neglect of chemistry in the model. If organic chemistry is twice as intense (i.e., $E^{norm}_{VOCs} = 2$), the site is very far from compliance, and reaching compliance would require reducing E_{NO_x} by ~25% or f_{NO_2} from 0.26 to 0.12, with concomitantly large implications for control technology and regulation. The compliance line shifts nonlinearly in terms of free-radical chemistry from the intense situation (dashed line) to the "*zero*" situation (dotted line) as E_{VOCs} are reduced, implying that reducing E_{VOCs} alone results in progressively less effective NO_2 mitigation, leading to a VOCs-saturated and NO_x-sensitive condition. Therefore, multi-variate synergistic controls (e.g., the oblique arrow in Fig. 1a, with a shorter distance between the IEC and the limitation) offer a more effective way of reducing NO_2 in street canyons. However, note that the optimum path for air quality amelioration varies significantly based on the geometry of canyons and should be evaluated carefully in each instance. The distance between the present emission scenario and the three-dimensional compliance surface may help stakeholders in designing more effective strategies for improving air quality in urban areas (e.g., Supplementary Fig. 2).

The situation is more complicated when the building height is doubled, as this greatly reduces the exchange velocity and increases the residence time of air pollutants, allowing more time for chemistry to take place[25,53]. For the deep canyon (Fig. 1b), E_{NO_x} requires to be reduced absolutely (~65%) as NO_2 is extremely high. Neglecting free-radical chemistry makes a very significant difference to modelled NO_2 and, hence, to the position of a site relative to the compliance line (dotted line in Fig. 1b). For our hypothetical deep London canyon, the NO_x reduction required would be underestimated by almost 50% for modelling that ignores chemistry (i.e., the dotted compliance line at $f_{NO_2} = 0.26$)

Table 1. The "wiggle room" (χ, dimensionless) under the hourly NO_2 compliance line[(a)].

E^{norm}_{VOCs}[(b)]	Regular canyon (AR = 1)			Deep canyon (AR = 2)		
	0.1	1.0	2.0	0.1	1.0	2.0
Case 0	1.89	1.82	1.48	0.73	0.24	0.29
Case 1[(c)]	1.46	0.78	0.54	0.41	0.16	0.22
Case 2[(c)]	>1.9[a]	>1.9[a]	>1.9[a]	1.01	0.34	0.32
Case 3[(d)]	1.87	1.80	1.43	0.71	0.24	0.28
Case 4[(d)]	1.86	1.77	1.39	0.69	0.23	0.27

[a]The maximum value for χ in the AR = 1 phase space is 1.9; higher values indicates that parameter values beyond the state space investigated would be compliant.
[b] E^{norm}_{VOCs} represents the ratio of VOC emission rates to its typical emission condition (TEC).
[c]Varying prevailing wind velocity.
[d]Varying distribution of vehicle emissions.

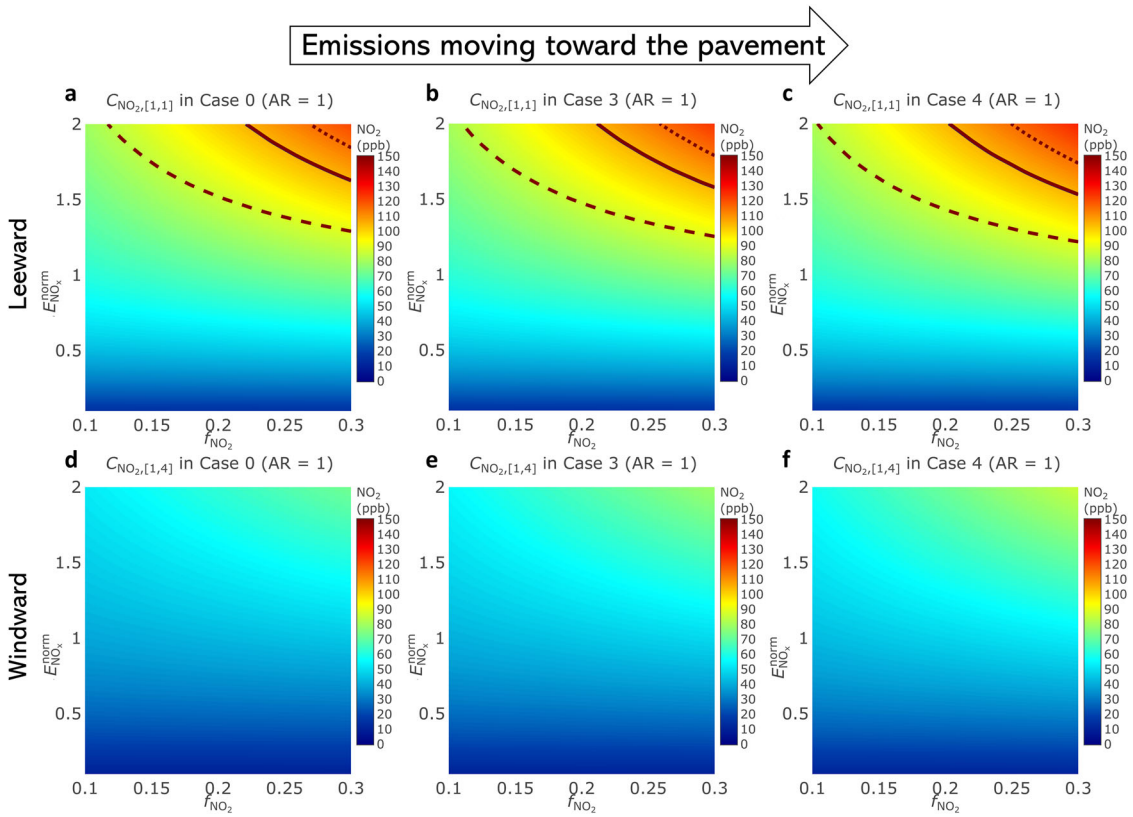

Fig. 2 Emission heterogeneities on NO_2 mixing-ratios in the regular canyon. The mixing-ratios (ppb) of NO_2 on the leeward side ($C_{NO_2,[1,1]}$) and windward side ($C_{NO_2,[1,4]}$) of the regular canyon at $E^{norm}_{VOCs} = 1$ under different emission heterogeneities. f_{NO_2} is the primary NO_2 fraction, and $E^{norm}_{NO_x}$ is the ratio of NO_x emission rates to the TEC of a typical emission condition. The solid line represents the UK air quality hourly NO_2 limit (105 ppb), and this contour line shifts to the dotted and dashed lines when E^{norm}_{VOCs} changes to 0.1 and 2, respectively.

and this underestimation gets markedly worse for lower values of f_{NO_2}.

The region "C" of compliant air quality in the two-dimensional E_{NO_x} — f_{NO_2} space (Fig. 1) can be thought of as comprising the "wiggle room" (χ) of different E_{NO_x} and f_{NO_2} scenarios that provided tolerable air quality in street canyons (see further discussion in Supplementary Discussion, subsection 4). When the compliance line is linear with respect to E_{NO_x}, region "C" is a simple shape (e.g., the solid and dashed lines in Fig. 1b) and air quality management options are simple to describe. When the compliance line is either not linear or becomes far apart for the different chemistry intensities (e.g., Fig. 1a), then visual inspection of phase space is the best way to consider management options.

Numerically integrating this region to calculate the area of compliant parameters collapses the complexity of Fig. 1a into a single number, but that number provides a useful metric for quantifying the effect of free-radical chemistry on in-canyon NO_2; the changing magnitude of χ reflects the sensitivity of NO_2 to key emission variables such as E_{NO_x} and E_{VOCs} (see Supplementary Discussion, subsection 4). The metric, χ, is computed as a dimensionless value of emissions in Table 1 within the 2D space of Fig. 1. The difference in the metric between the "low free-radical chemistry" scenario ($E^{norm}_{VOCs} = 0.1$) and the "intense free-radical chemistry" ($E^{norm}_{VOCs} = 2$) provides an upper limit to the extent to which neglect of free-radical chemistry overestimates the compliant phase space available in the street canyon, and so measures the potential for false positives in the regulatory modelling. For instance, introducing free-radical chemistry ($E^{norm}_{VOCs} = 1$) to the standard case, Case 0, decreases the air quality management "wiggle room", χ, by only ~3.5%, but introducing free-radical chemistry to the low wind speed case, Case 1, decreases χ by 46%. For the deep canyon, the effect of free-radical chemistry is between 60% and 70% for all wind speeds (Table 1).

The dotted ("low free-radical chemistry", $E^{norm}_{VOCs} = 0.1$) compliance line in the deep canyon is non-linear, that is, its gradient becomes steeper where f_{NO_2} is less than ~0.2. Recalling that the range of f_{NO_2} can come about by changing the fraction of gasoline-driven vehicles in the fleet, this non-linearity indicates that neglecting free-radical chemistry introduces a large error in χ for areas dominated by gasoline engines. When $E^{norm}_{VOCs} = 2$ in the deep canyon, conversion of NO_2 to organic nitrates and PAN (Supplementary Table 6, reaction 125) results in a slight increase in χ (Fig. 1b, Table 1). Supplementary Fig. 8 and Supplementary Fig 9 present the isopleths of the mixing ratio of PAN as a function of E_{NO_x} and E_{VOCs} at the pedestrian level in regular and deep canyons, respectively. Since the production of PAN cannot be simulated by a simple NO_x-O_3 cycle, ignoring free-radical chemistry may result in an underestimate of the significance of PAN in street canyons. The model results show a clear spatial distribution of PAN in regular and deep street canyons, respectively; high PAN concentrations in the presence of low NO_x and high VOC emissions imply that lowering NO_x must be accompanied by a concerted effort on VOC emissions to limit PAN production in the UCL. Additional information is available in Supplementary Methods (i.e., model sensitivity).

Model sensitivity

Sensitivity runs (Supplementary Fig. 4–5; Table 1) determine the impacts of prevailing wind velocity (U_0) on NO_2 mixing ratios. Air quality within the modelled urban canyons improves considerably, up to ~25%, with better ventilation, and deteriorates sharply, by up to ~60%, when U_0 is low (Supplementary Fig. 4–5). This

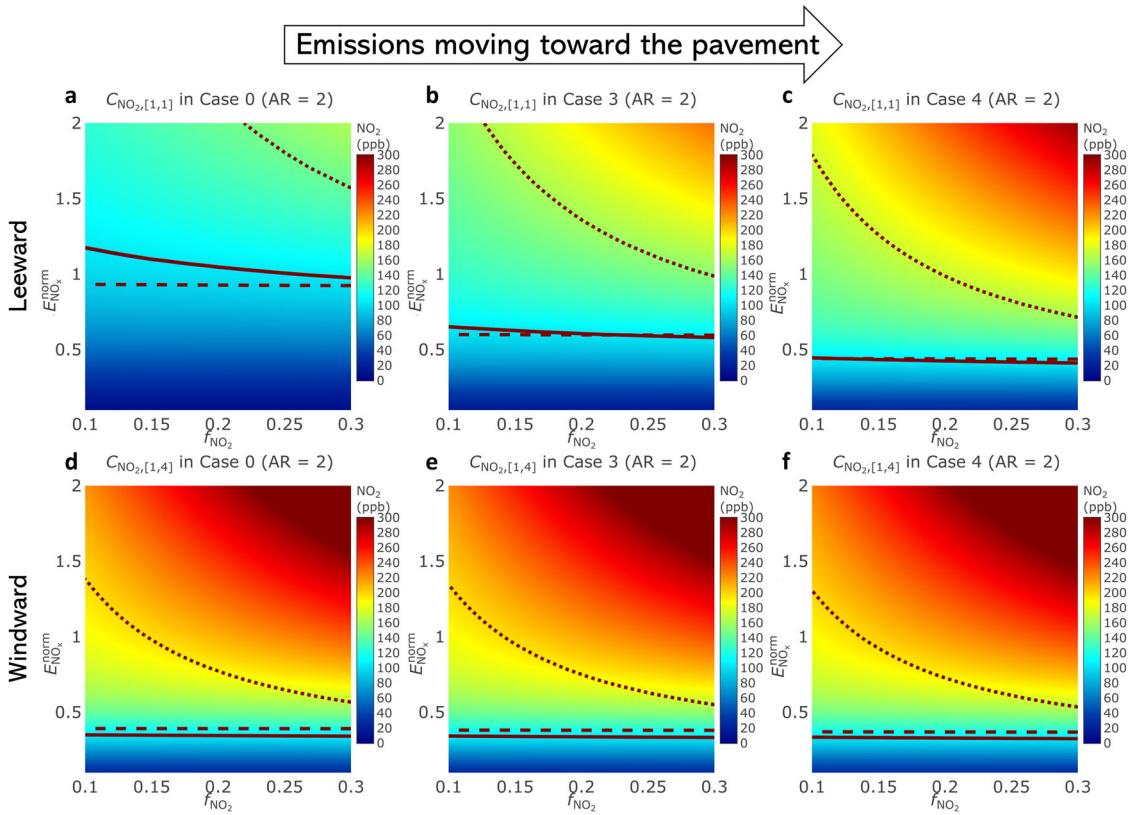

Fig. 3 Emission heterogeneities on NO_2 mixing-ratios in the deep canyon. The mixing-ratios (ppb) of NO_2 on the leeward side ($C_{NO_2,[1,1]}$) and windward side ($C_{NO_2,[1,4]}$) of the deep canyon at $E^{norm}_{VOCs} = 1$ under different emission heterogeneities. f_{NO_2} is the primary NO_2 fraction, and $E^{norm}_{NO_x}$ is the ratio of NO_x emission rates to the TEC of a typical emission condition. The solid line represents the UK air quality hourly NO_2 limit (105 ppb), and this contour line shifts to the dotted and dashed lines when E^{norm}_{VOCs} changes to 0.1 and 2, respectively.

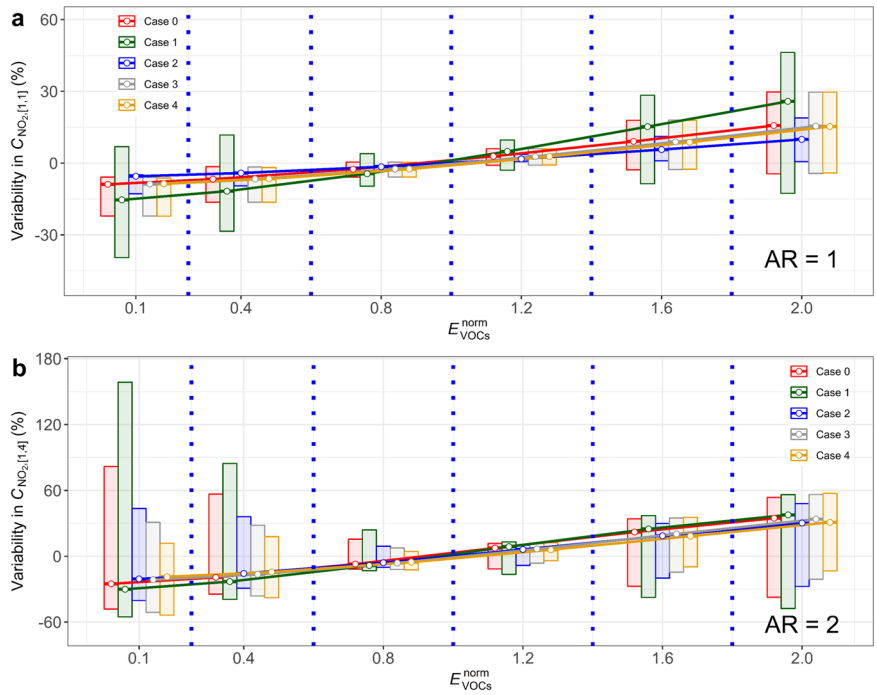

Fig. 4 The NO_2 variability under different emission scenarios. The variability in the mixing-ratio of NO_2 (%) under different normalised NO_x emissions ($E^{norm}_{NO_x}$), VOC emissions (E^{norm}_{VOCs}), and primary NO_2 fractions (f_{NO_2}) in regular (**a**) and deep (**b**) street canyons, respectively. Each area divided by a vertical blue dotted line represents one VOC emission scenario, as labelled. The points and solid lines represent the variability in NO_2 for the intense emission condition (IEC) on a putative perfect AR = 1 "Marylebone Road" ($E^{norm}_{NO_x} = 2$, $f_{NO_2} = 0.26$).

behavior is in line with previous modelling results[54] and observations[55]. In our model, the airflow inside street canyons is assumed to be linearly scaled to U_0, but the effects on NO_2 are highly non-linear with respect to emission profiles and monitoring locations within street canyons (Supplementary Fig. 6–7) because of the tight coupling of chemistry-transport processes. In the regular canyon, χ drops very rapidly in Case 1 compared to Case 0 (Table 1) because the low U_0 implies a longer residence time for air parcels, making free-radical chemistry more important.

Figure 2 and Fig. 3 show the effect of emission heterogeneity on NO_2 mixing ratios near the carriageway. The mixing-ratio of NO_2 shows little change ($\chi \approx$ that in Case 0) at the upward-vortex side as vehicle emissions shift from the central street toward the pavement, but it becomes very different at the downward-vortex side, especially in the deep canyon (see Supplementary Fig. 5). This asymmetry has clear implications for coordinated urban planning of transport and the built environment. The emission heterogeneity may also alter the mass fluxes escaping the canyons and, thus, the overall mixing-ratio of pollutants within canyons. This becomes even more important when the blocking effect of central barriers and the segregation impact are taken into account, which merits future investigation.

An alternative view of VOC free-radical chemistry effects is provided in Fig. 4, which is produced from NO_2-E_{VOCs} "slices" through the full NO_2–E_{VOCs}–E_{NO_x}– f_{NO_2} phase space. For clarity, we normalize the E_{VOCs} values to $E_{VOCs,TEC}$ (i.e., E^{norm}_{VOCs}) and normalize NO_2 mixing-ratios to their values at $E^{norm}_{VOCs} = 1$. Each area divided by vertical dotted lines represents one VOC emission scenario as labelled in Fig. 4. The range of boxes represents the variability in NO_2 (%) under different E_{NO_x} and f_{NO_2} conditions, and the points and lines represent the variability in NO_2 (%) for the IEC situation. Model errors that would occur from using the simple NO_x-O_3 scheme are closely approximated by the *y*-axis range of the boxes, and are highly dependent upon E_{NO_x}, E_{VOCs}, f_{NO_2}, and street canyon geometries. The degree of model error, due to using the simple chemistry, is not linearly related to these emission parameters due to the chemical complexity.

In Case 0, the effect of neglecting VOC free-radical chemistry underestimates NO_2 by 5.9% to 22.1% (8.8% for the IEC) in the regular canyon, and becomes even more significant (−51.3% to 30.9%, −25.2% for the IEC) in the deep canyon. Lowering U_0 greatly enhances the residence time of reactive species and increases the range of under- or over-estimation in NO_2 (Case 1), making free-radical chemistry more important even in the regular canyon (−39.5% to 6.9%, −15.4% for the IEC). The effect of emission heterogeneity on NO_2 is minor in the regular canyon (Cases 3 and 4) under most circumstance but cannot be ignored in the deep canyon (Fig. 4).

Implications for future regulatory practice and modelling

Chemical (and microphysical) complexities in street canyons have been accommodated using one- and 1D two-box models of street canyons to date[44,54,56]. The magnitude of underestimation or overestimation of NO_x and NO_2 levels by the typical one-box model is quantified in Supplementary Discussion (Subsection 2). The one-box model significantly under- and over-estimated mixing-ratios on the upward- and downward-vortex sides of street canyons, respectively (Supplementary Fig. 12). The inaccuracy varies with U_0 but is more strongly dependent on emission source strength and heterogeneity. In general, the one-box model performs closer to multi-box model results for NO_x in less polluted areas (i.e., low E_{NO_x} and E_{VOCs}), but its performance on reactive species such as NO_2 does not improve correspondingly, due to non-linear chemistry. Previous studies have built empirical equations that are derived from long-term in-situ observations[57–59] for NO_2 calculation from NO_x in some operational models (e.g., STREET[60], AEOLIUS[61], OSPM[62,63]). Our results, however, indicate that such data-driven correlations would vary substantially across sites based on emissions (see, for example, Supplementary Fig. 4–7) and should be used with care in

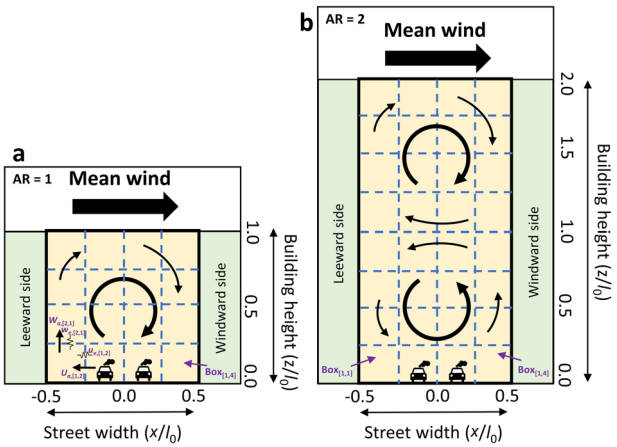

Fig. 5 A conceptual view of box models for regular and deep street canyons. The bold black frame represents a typical one-box model, the air is assumed to be well-mixed and thus, pollutants are homogeneously distributed; the dashed blue lines grided the single box into several compartments of equal volume, which represents 16- and 32-box models, respectively, in this example. A primary vortex exists within the regular canyon and two counter-rotated vortices exist within the deep canyon, the well-mixed assumption is applied for each box.

regulatory practice and modelling. An additional explanation is given in Supplementary Discussion (Subsection 3).

The results presented here, particularly our discussion of regulatory "wiggle room", χ, should not be interpreted as a tolerance of emissions, but rather as an acknowledgement that air quality management operates in the frame of available technologies and publicly acceptable regulation[21,64]. Although our focus has been on NO_2 and PAN, VOCs contribute significantly to the generation of other secondary pollutants such as O_3 and aerosols[65–67] and the management required to control those may be different. The impact of VOC free-radical chemistry on NO_2 concentrations in a regular canyon has been uncertain: it has been previously calculated to be rather limited (~10%)[26,68], or more significant[51]. By developing a computationally efficient model with spatial resolution and free-radical chemistry, we can draw out the impact of chemistry more clearly through an exploration of the model phase space. Our findings indicate that NO_2 production through VOC chemistry may be substantial or insignificant, depending in predictable ways on emission characteristics.

It is also worth noting that the effect of VOC chemistry on NO_2 at the pedestrian "hotspot" is likely much greater than the effect on the whole canyon volume. By focusing on "compliant" parameter sets producing model results below the UK 1-hour air quality standard, tens of thousands of model integrations can be described visually in a succinct way and even collapsed to a single integral metric, χ, which warns when neglect of radical chemistry is most misleading. The strong dependence of our results on aspect ratio and wind speed demonstrates starkly the need for emissions control given the densification of urban living[69,70] and the global terrestrial stilling (i.e., a reduction in land surface wind velocity of ~8%) which has been observed during recent decades[71–74].

Taking a broader perspective on the "wiggle room", this dimensionless factor can be used in a variety of more-or-less rigorous ways. Estimating the location of particular street canyons on the contour plot qualitatively is useful in order to develop efficient synergistic pathways for air quality regulations. The metric can be expanded to create a "wiggle volume" if necessary to fit in three-dimensional (3D) parameter space that can be explained in great detail (Supplementary Fig. 2). The local slope components of χ reflect the effectiveness of limiting a parameter (e.g., emissions) to improve air quality. Furthermore, χ could also be extended to be employed at larger scales, since cooperative control strategies for regional NO_x and VOC emissions are urgently needed, but research has not yet fully quantified their social costs[75,76].

METHODS

Model description

Figure 5 presents schematics of a typical one-box model and the multi-box models for street canyons with different geometries. The compartment with thick black lines represents the entire canyon (denoted by "Box_0") with a flat roof shape. The compartment overlying the building roofs represents the ambient background above the urban canopy layer (UCL). The canyon volume is split into several boxes (dashed blue lines) to give Eulerian grid resolutions of, in this case, "16-box" for the regular (AR = 1) canyon and "32-box" for the deep (AR = 2) canyon. Using the subscripts "k" pointing to the location along the ordinate direction and "i" to the location along the direction of the abscissa, the multi-box model can specify the position of any box within the canyon (denoted by "$Box_{[k,i]}$"). Assuming that a non-zero component of the ambient wind on the rooftop blows from left to right perpendicularly to the street axis, in-canyon boxes are indexed from the bottom-left, increasing upwards and rightwards (e.g., $k = 1$ represents the pedestrian level, and $i = 1$ represents model boxes near the leeward building facet). Emissions of NO_x (E_{NOx}) and VOCs (E_{VOCs}) from anthropogenic or natural sources can be injected into any box in the multi-box model. The mixing ratios of the qth species in Box_0 and in $Box_{[k,i]}$ are denoted as $C_{q,0}$ (ppb) and $C_{q,[k,i]}$ (ppb), respectively.

Turbulent mixing between the canyon and background is parameterized using "exchange rates" in the one- and multi-box models[24,44,48,77], respectively; in-canyon dynamics for the multi-box model comprise advection and turbulent diffusion, which are described by a set of parameters (Supplementary Tables 1–2), namely "advective velocity" and "turbulent velocity"[49]. These velocities are derived from previously computed LES data with the high Reynolds number (~10^6) turbulent airflow for idealised regular and deep canyons under a prevailing wind velocity (U_0) of 2 m s^{-1} in the neutral atmosphere[25,26], and a linear relationship is assumed for in-canyon dynamics with respect to U_0 in this study[78,79]. The mathematical description of the box models is presented in Supplementary Method (Subsection 1).

Modularization of the model code allows easy modification of chemical kinetics cell by cell for applications under complex scenarios (e.g., accounting for shaded areas or stagnant corners), and even the addition of particle microphysics instead of, or in addition to, gas-phase chemistry (cf., Zhong et al.[80]). In the present study, consistent chemical reaction rate coefficients are assumed within street canyons (i.e., one set of kinetic coefficients across the whole canyon). As with the calculation of the flow, there is a trade-off between computation time and the complexity of the chemical scheme. The chemical scheme should be as complicated as is required for the problem being studied, but not more complicated than necessary[77]. The near-explicit Master Chemical Mechanism (MCM)[81] or GECKO-A mechanism generator[82] could be used to provide a very detailed description of species-specific chemical evolution. To save computation time, we opt for a Reduced Chemical Scheme (RCS)[26] including 51 gas-phase species and 136 chemical reactions that was developed from a subset of the MCM *v*3.1 with comparable performance (~10%) against the full MCM *v*3.1 on NO, NO_2, O_3 and OH[26]. The RCS was used for simulating the daytime NO_x-O_3-VOC chemistry in the urban canyon environment by the multi-box models, and photolysis coefficients were calculated using the Tropospheric Ultraviolet and Visible (TUV) Radiation Model *v*4.1[83], representing for conditions during the

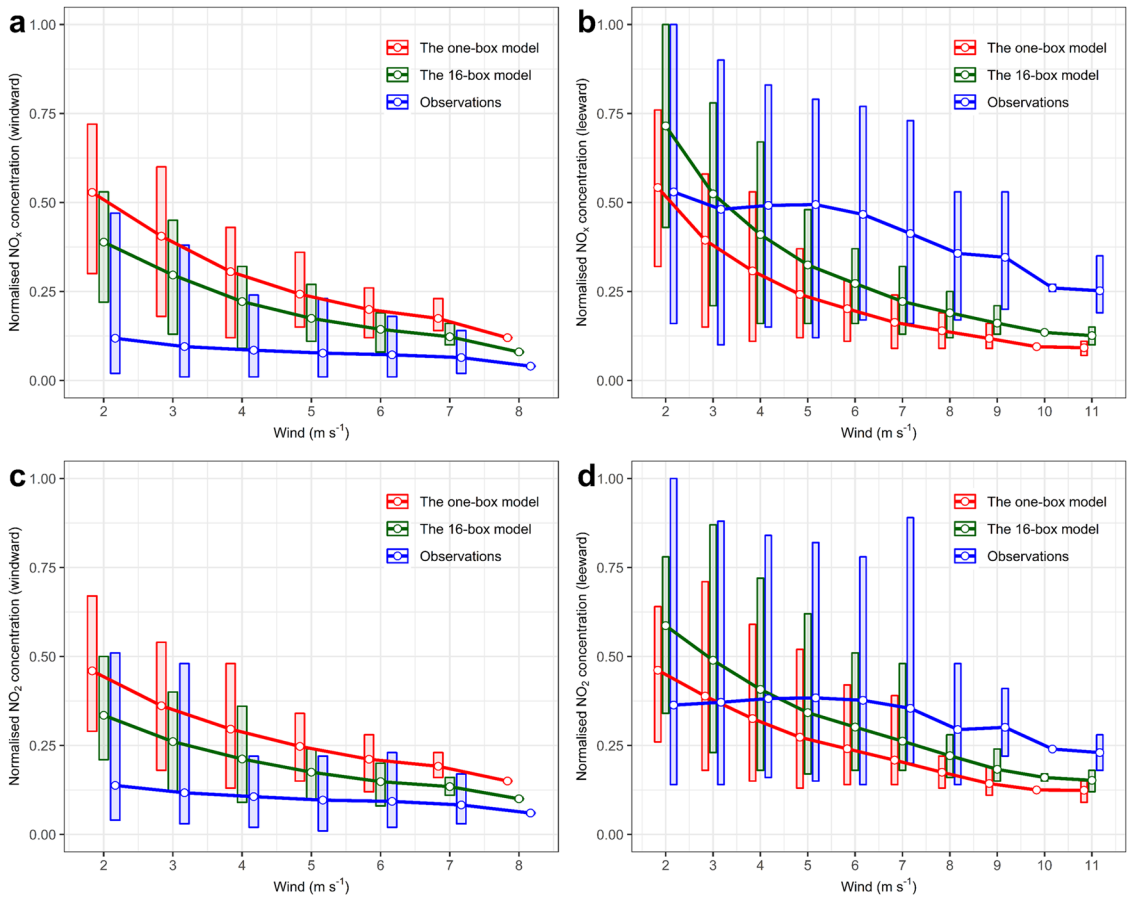

Fig. 6 Comparison of model results against observations. Comparison of normalized modelled NO_x and NO_2 concentrations against observations in Marylebone Road at various prevailing wind velocities (U_0) for the windward (**a**, **c**) and leeward (**b**, **d**) conditions. The error bars represent the range of data at the same U_0, and thus a similar airflow pattern within the street canyon. The points represent the average values for each group.

summer daytime in a typical street canyon at a mid-latitude urban area. Detailed information is provided elsewhere[26], and the full RCS mechanism including the chemical reaction rates is presented in Supplementary Tables 6–7. Compared to the simple inorganic NO_x-O_3 cycle, the somewhat more complicated chemistry of the RCS (i) incorporates the generation of NO_2 by reaction of NO with HO_2 and RO_2 (where R is an organic moiety); (ii) incorporates the production of organic nitrates and PAN; (iii) incorporates segregation; and (iv) allows some questions of VOC speciation to be addressed. Additionally, the RCS only considers gaseous chemistry and does not take into account heterogeneous reactions within street canyons, which is sufficient for our purposes in this work. However, our model indicates a potential pathway to investigate the effects of other chemistry on changes in air pollution by flexibly coupling specific chemical schemes.

Model evaluation

Having previously demonstrated that the passive tracer and NO_2 from the multi-box models matched well with those of the LES from which the flow was diagnosed[49], in this study, we evaluated the results of the one- and multi-box models against field observations. We use observations from the "Optimization of Modelling Methods for Traffic Pollution in Streets" (TRAPOS) — specifically from Schildhornstrasse (Berlin, Germany), Goettinger-strasse (Hanover, Germany), and Jagtvej (Copenhagen, Sweden) — and from Marylebone Road (UKA00315) and North Kensington (UKA00253) in central London, UK, which are parts of the national automatic monitoring network (AURN). The multi-box model with 16 in-canyon boxes performed well when evaluated using six widely-accepted metrics[84–87] (see Supplementary Table 5). Metrics from Hood et al.[88], which are representative of the state-of-art, are also provided; more information can be found in Supplementary Method (subsection 2).

Figure 6 presents a comparison of normalized modelled NO_x and NO_2 against observations (equation 20 in Supplementary Methods, subsection 2) under various prevailing wind velocities (U_0) in Marylebone Road, respectively. The 16-box model, in general, performed better with respect to NO_x and NO_2 compared to the typical one-box model due to its finer spatial resolution. For the windward condition (i.e., monitors located on the windward side of the canyon), modelled mixing ratios of NO_x and NO_2 were higher than observed values (Fig. 6a, c). As U_0 increased from 2 m s^{-1} to 8 m s^{-1}, modelled mixing ratios decreased significantly and monotonically, while observations dropped only slightly.

The pattern of model-measurement comparison may perhaps be explained by the fact that (1) the exchange velocity between the canyon and overlying background was much greater in reality than that used in the simulations because the monitoring cabinets in Marylebone Road are located where the actual AR of the canyon is less than unity, and the building roofs are rounded rather than rectangular; (2) the mechanical generation of turbulence overlying the UCL has been underestimated because the LES domain does not adequately represent the entire atmospheric boundary layer, resulting in the dynamics of the inner- and outer-layer being attenuated compared to reality[89].

As the exchange velocity increases, more recirculating pollutants are removed from the canyon. The effects of the background

Table 2. Summary of the multi-box model simulations for reactive species[a].

	Configuration
Case 0	$U_0 = 2.0\ m\ s^{-1}$; $1.0 \times (w_{e,0}, \lvert W_a, U_a \rvert, \lvert w_e, u_e \rvert)$; $\gamma_{q,[1,2]} = \gamma_{q,[1,3]} = 0.5$
Case 1	$U_0 = 1.2\ m\ s^{-1}$; $0.6 \times (w_{e,0}, \lvert W_a, U_a \rvert, \lvert w_e, u_e \rvert)$; $\gamma_{q,[1,2]} = \gamma_{q,[1,3]} = 0.5$
Case 2	$U_0 = 2.8\ m\ s^{-1}$; $1.4 \times (w_{e,0}, \lvert W_a, U_a \rvert, \lvert w_e, u_e \rvert)$; $\gamma_{q,[1,2]} = \gamma_{q,[1,3]} = 0.5$
Case 3	$U_0 = 2.0\ m\ s^{-1}$; $(w_{e,0}, \lvert W_a, U_a \rvert, \lvert w_e, u_e \rvert)$; $\gamma_{q,[1,1]} = \gamma_{q,[1,2]} = \gamma_{q,[1,3]} = \gamma_{q,[1,4]} = 0.25$
Case 4	$U_0 = 2.0\ m\ s^{-1}$; $(w_{e,0}, \lvert W_a, U_a \rvert, \lvert w_e, u_e \rvert)$; $\gamma_{q,[1,1]} = \gamma_{q,[1,4]} = 0.5$

[a]U_0: prevailing wind velocity in the background; $(w_{e,0}, \lvert W_a, U_a \rvert, \lvert w_e, u_e \rvert)$: in-canyon physical parameters for the multi-box models ($W_{a,[k,i]}$ and $U_{a,[k,i]}$ ($m\ s^{-1}$) are pollutant transfer velocities due to advective transportation respectively in the vertical and horizontal directions; and $w_{e,[k,i]}$ and $u_{e,[k,i]}$ ($m\ s^{-1}$) are transfer velocities due to turbulent mixing); $\gamma_{q,[1,i]}$ (i = 1, 2, 3, 4): the proportion of vehicle emissions in $Box_{[1,i]}$ to the total emissions (see Supplementary Methods). From Case 1 to Case 4, model sensitivities were conducted to investigate the effects of the prevailing wind, emission heterogeneity on in-canyon NO_2.

air become more important in determining mixing ratios of air pollutants on the windward side, which leads to a tendency for simulated and observed values to converge. For the leeward condition, observations exhibit very complex patterns (Fig. 6b, d) possibly due to the blocking effect of trees[90]. The box models remained sensitive to U_0; only a very slight decrease in wind speed was found in the observations. Consequently, the contrast between simulations and observations became larger under high U_0 scenarios. Supplementary Fig. 2 presents a comparison of normalized modelled NO_x against observations under different U_0 in three TRAPOS sites, respectively. While the 16-box model retains an advantage over the one-box model, the results show a substantial relationship between in-canyon concentrations and background wind velocities.

There are many potential sources of uncertainty complicating the comparison of models and observations, which are discussed in Supplementary Method (Subsection 2). We also note that adopting empirical parameters (Supplementary Table 4) for the multi-box model can compensate for such uncertainties and significantly improve the model performance for place-specific simulations (Supplementary Table 5, see Supplementary Methods for details). Overall, the multi-box model offers an improvement on the state-of-art for efficient simulation of the spatial distribution of reactive species within regular and deep canyons when tested against observations (Supplementary Table 5), current regulatory approaches (Supplementary Discussion, subsections 2 and 4) or the LES results[49].

Model scenarios

In this study, we neglect any complications induced by in-canyon vegetation, street furniture, heating or mechanical turbulence, and concentrate only on the same idealised (non-vegetated) regular and deep canyons as in previous studies[25,26]. Previous literature showed that NO_2 pollution was worst on the upward-vortex side at the pedestrian level of street canyons[25,26,38,91]. We therefore explore the variability of NO_2 mainly concentrating for the reporting of our results in these areas — that is, $C_{NO_2,[1,1]}$ for the regular canyon and $C_{NO_2,[1,4]}$ for the deep canyon (as illustrated in Fig. 5) — through a series of scenarios (Table 2). The spatial distribution of air pollutants in street canyons are provided in Supplementary Discussion, subsection 1.

We use an idealised Marylebone Road as our base regular street canyon (i.e., the building height and street width are 34 m), and then represent an idealised deep street canyon by doubling the building height to 68 m to investigate the effect of canyon geometry on pollutant mixing-ratios. As the primary driver for the ventilation of pollutants, the velocity of the prevailing wind (U_0) has significant impacts on air quality in street canyons, determining the intensity of vortices and, thus, the distribution of mixing-ratios within canyons; the emission heterogeneity may influence reactive species due to physical processes and segregation effects[92]. Taking a typical U_0 of $2\ m\ s^{-1}$, uniform emissions into the central carriageway ($Box_{[1,2]}$ and $Box_{[1,3]}$) and simple volume-splitting (i.e., boxes are equal in size) as the base case (Case 0), we performed model sensitivity studies (Case 1–4) to simulate the effect of U_0 (±40%) and to investigate crudely the impact of a central reservation or hedgerow on NO_2 in street canyons. Model results are discussed below, and details are presented in Supplementary Methods, subsection 3.

Initial conditions of NO, NO_2, O_3, and carbon monoxide (CO) were taken from in situ measurements at North Kensington (UKA00253) and were 2.6, 8.3, 32.0, and 151.4 ppb, respectively, representing a daytime summer atmosphere in London urban background for the year 2019. The model operated without any emissions for the first 30-minute "spin-up" period, which allowed sufficient time for turbulent dynamics to reach a quasi-equilibrium state for the preparation of key chemical intermediates[26,93], and the mixing ratios of all species at $t = 30$ min were used as background conditions. After the "spin-up" period, emissions were switched on and the multi-box model, as a representative of a typical urban unit, exchanges mass fluxes with the background continuously through the shear layer at the roof level. The averaged mixing ratios of pollutants at a quasi-equilibrium state (here $t = 180$–240 min) were used for analysis[54].

A typical emission condition (TEC) is defined with emission rates of 525.3, 1032.4, and 170.2 $g\ km^{-1}\ h^{-1}$ for NO_x, CO and VOCs, respectively, which represents a generic UK situation (i.e., not Marylebone Road) of weekday on-road traffic volume of 1500 vehicle hr^{-1} with an average speed of 40 $km\ hr^{-1}$ based on National Atmospheric Emissions Inventory (NAEI). The equivalent rates of emission of the qth species into a box grid is calculated as a mixing-ratio rate of change (denoted by "$E_{q,TEC}$"). We use a normalized emission rate (i.e., $E_q/E_{q,TEC}$, denoted by "E") to describe the variations in total emissions across the sensitivity study. It is assumed that the percentages of ethene (C_2H_4), propene (C_3H_6), formaldehyde (HCHO), and acetaldehyde (CH_3CHO) in the total VOC mix initially are 44%, 19%, 25%, and 12%, respectively, as calculated on the basis of annual mass emissions from road transport, photochemical ozone creation potential (POCP), and hydroxyl radical (OH) reactivity[26,94]. Although biogenic VOC emissions are not included in this research, they are expected to have a negligible effect on target pollutants such as NO_2 and PAN (see further discussion in Supplementary Method, subsection 3).

In each case, we model 8400 ($20 \times 20 \times 21$) emission scenarios in a trivariate space (i.e., $E^{norm}_{NO_x}$, E^{norm}_{VOCs}, primary NO_2 fractions (NO_2:NO_x, denoted by f_{NO_2})) where $E^{norm}_{NO_x} = 0.1, 0.2, \ldots, 1.9, 2.0$ and $E^{norm}_{VOCs} = 0.1, 0.2, \ldots, 1.9, 2.0$, reflecting tidal traffic volumes (150-3000 vehicles hr^{-1}, or equivalent emissions). Smaller values of E^{norm}_{VOCs} can also be interpreted as approaching the simple inorganic NO_x-O_3 cycle, and so also test the effect of VOC chemistry on the model results. The values of f_{NO_2} are lower in areas dominated by petrol engines but can be very high in megacities with large number of diesel engines[95], hence, $f_{NO_2} = 0.1, 0.11, \ldots, 0.29, 0.3$

can be interpreted as representing the efficiency of emissions control technology or, approximately, the effect of engine type on NO_2 in street canyons.

DATA AVAILABILITY

The observed air quality and weather data for the site on Marylebone Road in central London are available at https://uk-air.defra.gov.uk/networks/network-info?view=aurn; the data for the "Optimization of Modelling Methods for Traffic Pollution in Streets" (TRAPOS) sites are presented at https://www.dmu.dk/AtmosphericEnvironment/trapos/datadoc.htm.

CODE AVAILABILITY

The air quality multi-box modelling code for urban canyon simulations is given at https://github.com/YQ1229/MBOX4CANYON.

Received: 15 January 2022; Accepted: 1 December 2022;
Published online: 21 December 2022

REFERENCES

1. COMEAP. Available online: https://www.gov.uk/government/publications/nitrogen-dioxide-effects-on-mortality/associations-of-long-term-average-concentrations-of-nitrogen-dioxide-with-mortality-2018-comeap-summary (accessed on 24 August 2021) (2018).
2. World Health, O. Air pollution and child health: prescribing clean air: summary. (World Health Organization, 2018).
3. Zhang, X., Chen, X. & Zhang, X. The impact of exposure to air pollution on cognitive performance. *Proc. Natl Acad. Sci.* **115**, 9193–9197 (2018).
4. Kim, D., Chen, Z., Zhou, L.-F. & Huang, S.-X. Air pollutants and early origins of respiratory diseases. *Chronic Dis. Transl. Med.* **4**, 75–94 (2018).
5. Domingo, J. L. & Rovira, J. Effects of air pollutants on the transmission and severity of respiratory viral infections. *Environ. Res.* **187**, 109650 (2020).
6. LaFranchi, B. et al. Closing the peroxy acetyl nitrate budget: observations of acyl peroxy nitrates (PAN, PPN, and MPAN) during BEARPEX 2007. *Atmos. Chem. Phys.* **9**, 7623–7641 (2009).
7. Singh, H. B. & Hanst, P. L. Peroxyacetyl nitrate (PAN) in the unpolluted atmosphere: an important reservoir for nitrogen oxides. *Geophys. Res. Lett.* **8**, 941–944 (1981).
8. Davison, J. et al. Verification of a national emission inventory and influence of on-road vehicle manufacturer-level emissions. *Environ. Sci. Technol.* **55**, 4452–4461 (2021).
9. Valach, A., Langford, B., Nemitz, E., MacKenzie, A. R. & Hewitt, C. Seasonal and diurnal trends in concentrations and fluxes of volatile organic compounds in central London. *Atmos. Chem. Phys.* **15**, 7777–7796 (2015).
10. George, I. J. et al. Effects of cold temperature and ethanol content on VOC emissions from light-duty gasoline vehicles. *Environ. Sci. Technol.* **49**, 13067–13074 (2015).
11. Geng, F. et al. Analysis of VOC emissions using PCA/APCS receptor model at city of Shanghai, China. *J. Atmos. Chem.* **62**, 229–247 (2009).
12. Liu, Y. et al. Characteristics and sources of volatile organic compounds (VOCs) in Shanghai during summer: Implications of regional transport. *Atmos. Environ.* **215**, 116902 (2019).
13. Valach, A., Langford, B., Nemitz, E., MacKenzie, A. & Hewitt, C. Concentrations of selected volatile organic compounds at kerbside and background sites in central London. *Atmos. Environ.* **95**, 456–467 (2014).
14. Seco, R. et al. Contrasting winter and summer VOC mixing ratios at a forest site in the Western Mediterranean Basin: the effect of local biogenic emissions. *Atmos. Chem. Phys.* **11**, 13161–13179 (2011).
15. Sahu, L., Tripathi, N. & Yadav, R. Contribution of biogenic and photochemical sources to ambient VOCs during winter to summer transition at a semi-arid urban site in India. *Environ. Pollut.* **229**, 595–606 (2017).
16. McDonald, B. C., Dallmann, T. R., Martin, E. W. & Harley, R. A. Long-term trends in nitrogen oxide emissions from motor vehicles at national, state, and air basin scales. *J. Geophys. Res.: Atmos.* **117**, D21 (2012).
17. Fu, X. et al. High-resolution simulation of local traffic-related NO_x dispersion and distribution in a complex urban terrain. *Environ. Pollut.* **263**, 114390 (2020).
18. Veratti, G. et al. Towards the coupling of a chemical transport model with a micro-scale Lagrangian modelling system for evaluation of urban NO_x levels in a European hotspot. *Atmos. Environ.* **223**, 117285 (2020).
19. Good, N. et al. The Fort Collins Commuter Study: Impact of route type and transport mode on personal exposure to multiple air pollutants. *J. Exposure Sci. Environ. Epidemiol.* **26**, 397–404 (2016).
20. World Health, O. *WHO global air quality guidelines: particulate matter (PM2.5 and PM10), ozone, nitrogen dioxide, sulfur dioxide and carbon monoxide*. xxi, 267 p. (World Health Organization, 2021).
21. Joint Air Quality Unit. Improving Air Quality in the UK: Tackling Nitrogen Dioxide in Our Towns and Cities. *Department for Environment Food & Rural Affairs and Department for Transport: London, UK* (2017).
22. Cohen, B. Urbanization in developing countries: current trends, future projections, and key challenges for sustainability. *Technol. Soc.* **28**, 63–80 (2006).
23. Oke, T. R., Mills, G. & Voogt, J. *Urban Climates*. (Cambridge University Press, 2017).
24. Vardoulakis, S., Fisher, B. E., Pericleous, K. & Gonzalez-Flesca, N. Modelling air quality in street canyons: a review. *Atmos. Environ.* **37**, 155–182 (2003).
25. Zhong, J., Cai, X.-M. & Bloss, W. J. Modelling the dispersion and transport of reactive pollutants in a deep urban street canyon: using large-eddy simulation. *Environ. Pollut.* **200**, 42–52 (2015).
26. Bright, V. B., Bloss, W. J. & Cai, X. Urban street canyons: coupling dynamics, chemistry and within-canyon chemical processing of emissions. *Atmos. Environ.* **68**, 127–142 (2013).
27. Chew, L. W., Aliabadi, A. A. & Norford, L. K. Flows across high aspect ratio street canyons: Reynolds number independence revisited. *Environ. Fluid Mech.* **18**, 1275–1291 (2018).
28. Yang, H. et al. Numerical investigations of Re-independence and influence of wall heating on flow characteristics and ventilation in full-scale 2D street canyons. *Build. Environ.* **189**, 107510 (2021).
29. Zhang, K. et al. Numerical evaluations of urban design technique to reduce vehicular personal intake fraction in deep street canyons. *Sci. Total Environ.* **653**, 968–994 (2019).
30. Salizzoni, P., Soulhac, L. & Mejean, P. Street canyon ventilation and atmospheric turbulence. *Atmos. Environ.* **43**, 5056–5067 (2009).
31. Liu, C.-H. & Leung, D. Y. Numerical study on the ozone formation inside street canyons using a chemistry box model. *J. Environ. Sci.* **20**, 832–837 (2008).
32. Hewitt, C. N. & Jackson, A. V. *Handbook of atmospheric science: Principles and applications*. (John Wiley & Sons, 2008).
33. Baker, J., Walker, H. L. & Cai, X. A study of the dispersion and transport of reactive pollutants in and above street canyons—a large eddy simulation. *Atmos. Environ.* **38**, 6883–6892 (2004).
34. Lyu, X. et al. Causes of a continuous summertime O_3 pollution event in Jinan, a central city in the North China Plain. *Atmos. Chem. Phys.* **19**, 3025–3042 (2019).
35. Yang, G., Liu, Y. & Li, X. Spatiotemporal distribution of ground-level ozone in China at a city level. *Sci. Rep.* **10**, 1–12 (2020).
36. Wang, N. et al. Aggravating O_3 pollution due to NO_x emission control in eastern China. *Sci. Total Environ.* **677**, 732–744 (2019).
37. Tominaga, Y. & Stathopoulos, T. CFD modeling of pollution dispersion in a street canyon: Comparison between LES and RANS. *J. Wind Eng. Ind. Aerodyn.* **99**, 340–348 (2011).
38. Baik, J.-J., Kang, Y.-S. & Kim, J.-J. Modeling reactive pollutant dispersion in an urban street canyon. *Atmos. Environ.* **41**, 934–949 (2007).
39. Salim, S. M., Buccolieri, R., Chan, A. & Di Sabatino, S. Numerical simulation of atmospheric pollutant dispersion in an urban street canyon: Comparison between RANS and LES. *J. Wind Eng. Ind. Aerodyn.* **99**, 103–113 (2011).
40. Han, B.-S., Baik, J.-J., Kwak, K.-H. & Park, S.-B. Large-eddy simulation of reactive pollutant exchange at the top of a street canyon. *Atmos. Environ.* **187**, 381–389 (2018).
41. Wu, L., Hang, J., Wang, X., Shao, M. & Gong, C. APFoam 1.0: integrated computational fluid dynamics simulation of O 3–NO x–volatile organic compound chemistry and pollutant dispersion in a typical street canyon. *Geoscientific Model Dev.* **14**, 4655–4681 (2021).
42. Takano, Y. & Moonen, P. On the influence of roof shape on flow and dispersion in an urban street canyon. *J. Wind Eng. Ind. Aerodyn.* **123**, 107–120 (2013).
43. Murena, F., Favale, G., Vardoulakis, S. & Solazzo, E. Modelling dispersion of traffic pollution in a deep street canyon: application of CFD and operational models. *Atmos. Environ.* **43**, 2303–2311 (2009).
44. Pugh, T. A., MacKenzie, A. R., Whyatt, J. D. & Hewitt, C. N. Effectiveness of green infrastructure for improvement of air quality in urban street canyons. *Environ. Sci. Technol.* **46**, 7692–7699 (2012).
45. Vinuesa, J.-F. & de Arellano, J. V.-G. Introducing effective reaction rates to account for the inefficient mixing of the convective boundary layer. *Atmos. Environ.* **39**, 445–461 (2005).
46. Pugh, T. et al. The influence of small-scale variations in isoprene concentrations on atmospheric chemistry over a tropical rainforest. *Atmos. Chem. Phys.* **11**, 4121–4134 (2011).
47. Sykes, R., Parker, S., Henn, D. & Lewellen, W. Turbulent mixing with chemical reaction in the planetary boundary layer. *J. Appl. Meteorol. Climatol.* **33**, 825–834 (1994).

48. Soulhac, L., Salizzoni, P., Cierco, F.-X. & Perkins, R. The model SIRANE for atmospheric urban pollutant dispersion; part I, presentation of the model. *Atmos. Environ.* **45**, 7379–7395 (2011).
49. Dai, Y., Cai, X., Zhong, J. & MacKenzie, A. R. Modelling chemistry and transport in urban street canyons: comparing offline multi-box models with large-eddy simulation. *Atmos. Environ.* **264**, 118709 (2021).
50. Kwak, K.-H. & Baik, J.-J. A CFD modeling study of the impacts of NO_x and VOC emissions on reactive pollutant dispersion in and above a street canyon. *Atmos. Environ.* **46**, 71–80 (2012).
51. Kim, M. J., Park, R. J. & Kim, J.-J. Urban air quality modeling with full O_3–NO_x–VOC chemistry: Implications for O_3 and PM air quality in a street canyon. *Atmos. Environ.* **47**, 330–340 (2012).
52. Kwak, K.-H., Baik, J.-J. & Lee, K.-Y. Dispersion and photochemical evolution of reactive pollutants in street canyons. *Atmos. Environ.* **70**, 98–107 (2013).
53. Park, S.-J., Kim, J.-J., Kim, M. J., Park, R. J. & Cheong, H.-B. Characteristics of flow and reactive pollutant dispersion in urban street canyons. *Atmos. Environ.* **108**, 20–31 (2015).
54. Zhong, J., Cai, X.-M. & Bloss, W. J. Modelling photochemical pollutants in a deep urban street canyon: application of a coupled two-box model approximation. *Atmos. Environ.* **143**, 86–107 (2016).
55. Gidhagen, L., Johansson, C., Langner, J. & Olivares, G. Simulation of NO_x and ultrafine particles in a street canyon in Stockholm, Sweden. *Atmos. Environ.* **38**, 2029–2044 (2004).
56. Nikolova, I., MacKenzie, A. R., Cai, X., Alam, M. S. & Harrison, R. M. Modelling component evaporation and composition change of traffic-induced ultrafine particles during travel from street canyon to urban background. *Faraday Discuss.* **189**, 529–546 (2016).
57. Kakosimos, K. E., Hertel, O., Ketzel, M. & Berkowicz, R. Operational Street Pollution Model (OSPM)–a review of performed application and validation studies, and future prospects. *Environ. Chem.* **7**, 485–503 (2010).
58. Westmoreland, E. J., Carslaw, N., Carslaw, D. C., Gillah, A. & Bates, E. Analysis of air quality within a street canyon using statistical and dispersion modelling techniques. *Atmos. Environ.* **41**, 9195–9205 (2007).
59. Masey, N., Hamilton, S. & Beverland, I. J. Development and evaluation of the RapidAir® dispersion model, including the use of geospatial surrogates to represent street canyon effects. *Environ. Model. Softw.* **108**, 253–263 (2018).
60. Johnson, W., Ludwig, F., Dabberdt, W. & Allen, R. An urban diffusion simulation model for carbon monoxide. *J. Air Pollut. Control Assoc.* **23**, 490–498 (1973).
61. Buckland, A. & Middleton, D. Nomograms for calculating pollution within street canyons. *Atmos. Environ.* **33**, 1017–1036 (1999).
62. Berkowicz, R. OSPM-A parameterised street pollution model. *Environ. Monit. Assess.* **65**, 323–331 (2000).
63. Vardoulakis, S., Valiantis, M., Milner, J. & ApSimon, H. Operational air pollution modelling in the UK—Street canyon applications and challenges. *Atmos. Environ.* **41**, 4622–4637 (2007).
64. DEFRA. *Clean air strategy 2019*. Department for Environment Food & Rural Affairs and Department for Transport: London, UK (2019).
65. Mozaffar, A., Zhang, Y.-L., Fan, M., Cao, F. & Lin, Y.-C. Characteristics of summertime ambient VOCs and their contributions to O_3 and SOA formation in a suburban area of Nanjing, China. *Atmos. Res.* **240**, 104923 (2020).
66. Wu, R. & Xie, S. Spatial distribution of ozone formation in China derived from emissions of speciated volatile organic compounds. *Environ. Sci. Technol.* **51**, 2574–2583 (2017).
67. Wang, P., Chen, Y., Hu, J., Zhang, H. & Ying, Q. Attribution of tropospheric ozone to NO_x and VOC emissions: considering ozone formation in the transition regime. *Environ. Sci. Technol.* **53**, 1404–1412 (2018).
68. Garmory, A., Kim, I., Britter, R. & Mastorakos, E. Simulations of the dispersion of reactive pollutants in a street canyon, considering different chemical mechanisms and micromixing. *Atmos. Environ.* **43**, 4670–4680 (2009).
69. Næss, P., Saglie, I.-L. & Richardson, T. Urban sustainability: is densification sufficient? *Eur. Plan. Stud.* **28**, 146–165 (2020).
70. Stone, B. Jr., Mednick, A. C., Holloway, T. & Spak, S. N. Is compact growth good for air quality? *J. Am. Plan. Assoc.* **73**, 404–418 (2007).
71. Zeng, Z. et al. A reversal in global terrestrial stilling and its implications for wind energy production. *Nat. Clim. Change* **9**, 979–985 (2019).
72. Vautard, R., Cattiaux, J., Yiou, P., Thépaut, J.-N. & Ciais, P. Northern Hemisphere atmospheric stilling partly attributed to an increase in surface roughness. *Nat. Geosci.* **3**, 756–761 (2010).
73. Tian, Q., Huang, G., Hu, K. & Niyogi, D. Observed and global climate model based changes in wind power potential over the Northern Hemisphere during 1979–2016. *Energy* **167**, 1224–1235 (2019).
74. McVicar, T. R., Roderick, M. L., Donohue, R. J. & Van Niel, T. G. Less bluster ahead? Ecohydrological implications of global trends of terrestrial near-surface wind speeds. *Ecohydrology* **5**, 381–388 (2012).
75. Shen, H. et al. Novel method for ozone isopleth construction and diagnosis for the ozone control strategy of Chinese cities. *Environ. Sci. Technol.* **55**, 15625–15636 (2021).
76. Ding, D. et al. Optimization of a NO_x and VOC cooperative control strategy based on clean air benefits. *Environ. Sci. Technol.* **56**, 739–749 (2021).
77. Zhong, J., Cai, X.-M. & Bloss, W. J. Coupling dynamics and chemistry in the air pollution modelling of street canyons: a review. *Environ. Pollut.* **214**, 690–704 (2016).
78. Murena, F., Di Benedetto, A., D'Onofrio, M. & Vitiello, G. Mass transfer velocity and momentum vertical exchange in simulated deep street canyons. *Bound. -Layer. Meteorol.* **140**, 125–142 (2011).
79. Barlow, J. F., Harman, I. N. & Belcher, S. E. Scalar fluxes from urban street canyons. Part I: Laboratory simulation. *Bound.-Layer. Meteorol.* **113**, 369–385 (2004).
80. Zhong, J., Nikolova, I., Cai, X., MacKenzie, A. R. & Harrison, R. M. Modelling traffic-induced multicomponent ultrafine particles in urban street canyon compartments: Factors that inhibit mixing. *Environ. Pollut.* **238**, 186–195 (2018).
81. Saunders, S. M., Jenkin, M. E., Derwent, R. & Pilling, M. Protocol for the development of the Master Chemical Mechanism, MCM v3 (Part A): tropospheric degradation of non-aromatic volatile organic compounds. *Atmos. Chem. Phys.* **3**, 161–180 (2003).
82. Aumont, B., Szopa, S. & Madronich, S. Modelling the evolution of organic carbon during its gas-phase tropospheric oxidation: development of an explicit model based on a self generating approach. *Atmos. Chem. Phys.* **5**, 2497–2517 (2005).
83. Madronich, S. & Flocke, S. The Role of Solar Radiation in Atmospheric Chemistry. In: Boule, P. (eds) *Environmental Photochemistry*. **2**, 1–26 (1999).
84. Cai, X.-M. & Steyn, D. Modelling study of sea breezes in a complex coastal environment. *Atmos. Environ.* **34**, 2873–2885 (2000).
85. Willmott, C. J. et al. Statistics for the evaluation and comparison of models. *J. Geophys. Res.: Oceans* **90**, 8995–9005 (1985).
86. Willmott, C. J. On the validation of models. *Phys. Geogr.* **2**, 184–194 (1981).
87. Willmott, C. J., Robeson, S. M. & Matsuura, K. A refined index of model performance. *Int. J. Climatol.* **32**, 2088–2094 (2012).
88. Hood, C. et al. Comprehensive evaluation of an advanced street canyon air pollution model. *J. Air Waste Manag. Assoc.* **71**, 247–267 (2021).
89. Grylls, T., Suter, I. & van Reeuwijk, M. Steady-state large-eddy simulations of convective and stable urban boundary layers. *Bound. -Layer. Meteorol.* **175**, 309–341 (2020).
90. Buccolieri, R., Jeanjean, A. P., Gatto, E. & Leigh, R. J. The impact of trees on street ventilation, NO_x and PM2. 5 concentrations across heights in Marylebone Rd street canyon, central London. *Sustain. Cities Soc.* **41**, 227–241 (2018).
91. Moradpour, M., Afshin, H. & Farhanieh, B. A numerical investigation of reactive air pollutant dispersion in urban street canyons with tree planting. *Atmos. Pollut. Res.* **8**, 253–266 (2017).
92. Zhong, J., Cai, X.-M. & Bloss, W. J. Modelling segregation effects of heterogeneous emissions on ozone levels in idealised urban street canyons: using photochemical box models. *Environ. Pollut.* **188**, 132–143 (2014).
93. Cai, X.-M., Barlow, J. & Belcher, S. Dispersion and transfer of passive scalars in and above street canyons—large-eddy simulations. *Atmos. Environ.* **42**, 5885–5895 (2008).
94. Boulter, P., Barlow, T., Latham, S. & McCrae, I. Emission factors 2009: Report 1-a review of methods for determining hotexhaust emission factors for road vehicles. *TRL Published Project Report* (2009).
95. Carslaw, D. C., Murrells, T. P., Andersson, J. & Keenan, M. Have vehicle emissions of primary NO_2 peaked? *Faraday Discuss.* **189**, 439–454 (2016).

ACKNOWLEDGEMENTS

The authors thank the University of Birmingham's BlueBEAR HPC service (http://www.bear.bham.ac.uk) for offering high-performance computational resource. We thank Dr. Vivian Bright for providing the reduced chemical scheme (RCS). A.R.M.K. thanks the UK Natural Environment Research Council for support through grants NE/S00582X/1 and NE/S003487/1.

AUTHOR CONTRIBUTIONS

Y.D. and A.R.M.K. wrote the paper. Y.D. designed the study and performed the analysis. J.Z. and X.C. performed the underlying LES model simulations. All authors reviewed and commented on the paper.

COMPETING INTERESTS

The authors declare no competing interests.

ADDITIONAL INFORMATION

Supplementary information The online version contains supplementary material available at https://doi.org/10.1038/s41612-022-00323-w.

Correspondence and requests for materials should be addressed to A. Robert MacKenzie.

Reprints and permission information is available at http://www.nature.com/reprints

Publisher's note Springer Nature remains neutral with regard to jurisdictional claims in published maps and institutional affiliations.